TSL-Note-2004-60

Comparison of Non-Linear Effects from the Electric Field of Several Current Distributions

Volker Ziemann
The Svedberg Laboratory, Uppsala University
75121 Uppsala, Sweden

Abstract

New electron coolers are equipped with electron guns that can create parabolic or hollow beams. With their corresponding electric field this may have a detrimental influence on the stability of the ion beam and lead to "electron heating." Here we investigate the effect of the transverse electric field of the electron beam in an electron cooler on an ion beam for different transverse current distributions.

PACS: 29.27.Bd

Uppsala, Sweden
December 2, 2004

Comparison of Non-Linear Effects from the Electric Field of Several Current Distributions

Volker Ziemann
The Svedberg Laboratory at Uppsala University
75121 Uppsala, Sweden

December 2, 2004

Abstract

New electron coolers are equipped with electron guns that can create parabolic or hollow beams. With their corresponding electric field this may have a detrimental influence on the stability of the ion beam and lead to "electron heating." Here we investigate the effect of the transverse electric field of the electron beam in an electron cooler on an ion beam for different transverse current distributions.

1 Introduction

In ref. [1] it is proposed to equip the electron cooler for the HESR ring in the FAIR facility [2] at GSI in Darmstadt, Germany with an electron gun that will allow the transverse profile of the electron current to be varied such that peaked, flat, and hollow beams are possible. A similar electron gun is also part of the new electron cooler in Lanzhou, China [3]. The reason for having e.g. a hollow beam is to avoid over-cooling the core of the ion beam which can lead to coherent instabilities. On the other hand, special transverse electron current distributions will create transverse electric fields that cause the ion beam to be kicked transversely. Considering the complex radial behavior of the electric field we can expect non-linear effects such as amplitude dependent tune-shift and driving non-linear resonance to become important. It is conjectured [4, 5] that these non-linear effects are the reason for "electron heating" observed in CELSIUS [4].

This report will first discuss several different distributions and the associated electric fields. We perform the same analysis that was done in Ref. [6] for these distributions and calculate the tune-shift with amplitude, the tune footprint and the corresponding resonance strengths. Finally we discuss our findings and their implication for future cooler projects.

2 Charge Distributions and Fields

In this report we compare the effect of four different charge distributions, namely

- Gaussian with rms σ,
- Parabolic with half width b,
- Hollow beam parabolic with radius b and ring width $a = 0.1\,b$,
- Erfc-distribution with radius b and transition width $a = 0.01\,b$.

In the calculations we choose the width parameter b to be equal to the width of the Gaussian distribution σ. Moreover, we normalize the distributions with respect to the measure $\int_0^\infty 2\pi r dr$, such that they contain equal numbers of particles, i.e. the current of the different distributions is equal. The distributions, with the proper normalization, are shown in Fig. 1 and the details of the parameterization and normalization of the distributions is deferred to the appendix.

The transverse kick that a proton at radius R receives is proportional to the electric field $E(R)$ which can be calculated from Gauss' law according to

$$2\pi R E(R) = \int_0^R 2\pi r \psi(r) dr \ . \tag{1}$$

We ignore constants for the time being, because we are interested in the relative effects between the four distributions. This expression is evaluated for the different distributions in the appendix and the corresponding curves are shown in Fig. 2. Note that the distributions that cause these electric fields contain identical numbers of particles.

Already from the electric fields we can draw several conclusions. First we note, that all curves agree for large amplitudes. This is a consequence of Gauss' law and the requirement that all distributions contain equal numbers of particles. Second, we note that the slope at the origin of the parabolic distribution is steepest, which will cause the largest tune shift. This is not surprising, because from Fig. 1 we know that the charge density at the origin is largest for the parabolic distribution and Gauss' law causes the field to be largest. The slope of the Erfc-distribution is only slightly smaller than that of the parabolic distribution. Third, we observe that there is zero field inside the hollow beam and the tune-shift at small amplitudes will vanish.

We can also observe that the Gaussian distribution is smoothest and that the hollow-beam distribution exhibits a very spiked behavior near the edge of the beam. We expect that to cause significantly enhanced excitation of non-linear resonances. We will investigate this effect closer in a later section.

3 Non-linear Tune-shift

In order to calculate the non-linear tune shift we mimic the calculations in ref. [6] and start with the differential equation for the transverse betatron motion with a single located non-linear force $\tilde{S}(\eta)$

$$\frac{d^2\eta}{d\theta^2} + \nu^2\eta = -4\pi\nu\tilde{S}(\eta)\delta_p(\theta) \tag{2}$$

where θ is the azimuthal variable and runs from zero to 2π. For a simple linear force we would have $\tilde{S}(\eta) = \xi\eta$, where ξ is the linear tune shift parameter. As independent variables we have chosen those of normalized phase space η, η' which are related to those of phase space x, x' and of action angle variables J, ϕ by

$$x = \sqrt{\beta_x}\eta = \sqrt{2J\beta_x}\cos(\phi) \quad \text{and} \quad \eta' = -\nu\sqrt{2J}\sin(\phi)\ . \tag{3}$$

In the next step we transform the equation of motion, eq. 2 to action-angle variables J, ϕ given by

$$2J = \eta^2 + (\eta'/\nu)^2 \quad \text{and} \quad \phi = -\arctan(\eta'/\nu\eta)\ . \tag{4}$$

The equation of motion for those variables now read

$$\begin{aligned}
\frac{dJ}{d\theta} &= \eta\eta' + \eta'\eta''/\nu^2 = -\frac{4\pi\eta'}{\nu}\tilde{S}(\eta)\delta_p(\theta) \\
&= 4\pi\sqrt{2J}\sin(\phi)\,\tilde{S}(\sqrt{2J}\cos\phi)\delta_p(\theta) \\
\frac{d\phi}{d\theta} &= \frac{-1}{1+(\eta'/\nu\eta)^2}\left\{\frac{\eta''}{\nu\eta} - \frac{\eta'^2}{\nu\eta^2}\right\} \\
&= \frac{-1}{1+\tan^2\phi}\left\{-\nu(1+\tan^2\phi) - \frac{4\pi}{\eta}\tilde{S}(\eta)\delta_p(\theta)\right\} \\
&= \nu + \frac{4\pi\cos\phi}{\sqrt{2J}}\tilde{S}(\sqrt{2J}\cos\phi)\delta_p(\theta)
\end{aligned} \tag{5}$$

The non-linear tune shift can be calculated by averaging the right hand side of the equation for $d\phi/d\theta$ over θ. This amounts to replacing the delta-function by $1/2\pi$ and by averaging over the phase variable ϕ. We thus arrive at

$$\Delta\nu(J) = \frac{2}{\sqrt{2J}}\int_0^{2\pi}\frac{d\phi}{2\pi}\cos\phi\tilde{S}(\sqrt{2J}\cos\phi)\ . \tag{6}$$

As a check we calculate the tune shift for a constant linear force $\tilde{S}(\eta) = \xi\eta$. It is easy to see that in this case the tune shift ξ is recovered. For the round-beam beam-beam kick $2\sigma^2(1-e^{-x^2/2\sigma^2})/x)$ the integral can be evaluated in terms of Bessel functions [7]. For a general kick $\tilde{S}$, however, it is easiest to evaluate the

integral numerically which is what we do for the four distributions and show the results in Fig. 3.

Here we see that the parabolic distribution indeed has the largest slope followed by the erfc distribution. The Gaussian distribution and the hollow beam distribution would only cause a tune-shift on the order of a quarter of that of the parabolic distribution with the same total current.

4 Tune Footprint

The tune-shift calculated in the previous section is only valid for one-dimensional motion if, for example, one of the transverse emittances is zero. Here we will drop this restriction and calculate the tune footprint for two-dimensional betatron oscillations with unequal Courant-Snyder invariants J_x and J_y.

In this case the equations of motion for the coupled system in x and y read

$$\begin{aligned} \frac{d^2\eta_x}{d\theta^2} + \nu_x^2\eta_x &= -4\pi\nu_x\tilde{S}(r)\frac{\eta_x}{r}\delta_p(\theta) \\ \frac{d^2\eta_y}{d\theta^2} + \nu_y^2\eta_y &= -4\pi\nu_y\tilde{S}(r)\frac{\eta_y}{r}\delta_p(\theta) \\ \text{with} \quad r^2 &= 2J_x\cos^2\phi_x + 2J_y\cos^2\phi_y \end{aligned} \tag{7}$$

where η, η', ϕ, and J now carry subscripts x or y. Performing the same algebra that led to eq. 5 we obtain

$$\frac{d\phi_x}{d\theta} = \nu_x + 4\pi\cos^2\phi_x\frac{\tilde{S}(r)}{r}\delta(\theta) \tag{8}$$

and a similar equation for the vertical coordinate, labeled y. We now keep only the constant part of the delta-function, average over phases ϕ_x and ϕ_y, and reach

$$\Delta\nu_x(J_x, J_y) = 2\int_0^{2\pi}\frac{d\phi_x}{2\pi}\int_0^{2\pi}\frac{d\phi_y}{2\pi}\cos^2\phi_x\frac{\tilde{S}(\sqrt{2J_x\cos^2\phi_x + 2J_x\cos^2\phi_x})}{\sqrt{2J_x\cos^2\phi_x + 2J_x\cos^2\phi_x}} \tag{9}$$

and a similar equation for x and y exchanged. The double integral can be easily integrated numerically and we can plot the tune shifts $\Delta\nu_x$ and $\Delta\nu_y$ for different action variables J_x and J_y, as shown in Fig. 4 for the four distributions.

The top row of Fig. 4 shows the tune footprint for the parabolic and the Gaussian distribution, the bottom row the Erfc and the hollow-beam distribution. Again we observe that the extent of the tune excursion is largest for the parabolic distribution and somewhat smaller for the Erfc-distribution. The footprints for the Gaussian and hollow-beam are smallest. It is noteworthy, that the footprint of the hollow-beam is folded in the sense that the tune-shift for small and large amplitudes is zero and intermediate values have larger tune-shift. All other distributions have the largest tune-shift in the center of the electron beam

which then decreases for larger Courant-Snyder invariants J_x and J_y. Note that a large tune footprint will cause the beam to spread over a large area in the tune diagram, thus increasing the chance for resonant particle losses provided that the resonances are excited by either magnetic imperfections or the electron beam itself.

5 Resonances

Apart from causing the non-linear tune shift the electric field of the cooler also drives resonances, just as the beam-beam kick does in colliders. The resonance driving terms can be evaluated by following ref. [6] again. To this end we replace the periodic delta function in eq. 5 by its Fourier expansion

$$\delta_p(\theta) = \frac{1}{2\pi} \sum_{m=-\infty}^{\infty} e^{-im\theta} \ . \tag{10}$$

For $dJ/d\theta$ and $d\phi/d\theta$ we obtain the expressions

$$\begin{aligned} \frac{dJ}{d\theta} &= 2\sqrt{2J}\sin\phi\,\tilde{S}(\sqrt{2J}\cos\phi) \sum_{m=-\infty}^{\infty} e^{-im\theta} \\ \frac{d\phi}{d\theta} &= \nu + \frac{2\cos\phi}{\sqrt{2J}}\tilde{S}(\sqrt{2J}\cos\phi) \sum_{m=-\infty}^{\infty} e^{-im\theta} \ . \end{aligned} \tag{11}$$

We now consider the equation for ϕ and express the electric cooler profile function $\tilde{S}(\sqrt{2J}\cos\phi)$ as a Fourier series

$$\sqrt{2J}\cos\phi\,\tilde{S}(\sqrt{2J}\cos\phi) = J\sum_{n=0}^{\infty} A_n \cos n\phi \tag{12}$$

where the (action $J-$dependent) Fourier coefficients $A_n(J)$ can be easily calculated numerically by FFT [8]. The factor J is retained on the right hand side to make later formulae easier to write. Note that no sine-like terms, only cosine terms appear in that Fourier series, because any power series of $\cos\phi$ can be expressed in terms of $\cos n\phi$, only. After a little algebra we obtain

$$\begin{aligned} \frac{d\phi}{d\theta} &= \nu + \frac{\xi}{2}\sum_{n=0}^{\infty}\sum_{m=-\infty}^{\infty} A_n\left(\cos(n\phi - m\theta) + \cos(n\phi + m\theta)\right) \\ &= \nu + \xi\sum_{n=0}^{\infty} A_n \sum_{m=-\infty}^{\infty}\cos(n\phi - m\theta) \ . \end{aligned} \tag{13}$$

Now we are in a position to choose a single resonant phase χ given by $\chi = p\phi - q\theta$ and retain terms of the form $\cos(l(p\phi - q\theta)) = \cos l\chi$

$$\frac{d\phi}{d\theta} \approx \nu + \xi\sum_{l=0}^{\infty} A_{lp}\cos l\chi \tag{14}$$

Following ref. [6] we limit ourselves to $l = 0$ and 1 and can write

$$\frac{d\phi}{d\theta} \approx \nu + \xi \left(A_0 + A_p \cos\chi\right) = \nu + \xi A_0 + \xi A_p \cos\chi \tag{15}$$

Finally we change variables from ϕ to χ and get

$$\frac{d\chi}{d\theta} \approx (p\nu - q) + p\xi A_0 + p\xi A_p \cos p\chi \ . \tag{16}$$

In eq. 16 we recover the non-linear tune shift term A_0 which depends on the action variable J. From eq. 12 it is clear that inserting a linear force $\tilde{S}(\eta) = \eta$ with $A_0 = 1$ in eq. 16, we obtain the normal tune shift ξ, as expected. We also see that the "instantaneous tune" $d\phi/d\theta$ varies slowly in the vicinity of a resonance p/q with amplitude given by ξA_p which coincides with the definition of the resonance width in ref. [6].

In Fig. 5 we display the logarithm of the resonance strength A_p as a function of the Courant-Snyder invariant J for the distributions under consideration. In the top row we show the results for parabolic and Gaussian, in the bottom row for the Erfc and hollow-beam distributions. We observe that the Gaussian distribution causes the smoothest an also the weakest dependence on the action variable and that the driving terms for the higher orders are suppressed considerably. The driving terms for the parabolic distribution show a similar behavior, albeit a somewhat higher excitation near the edge of the distribution. The distributions in the bottom row of Fig. 5 which have the sharpest edges depict considerably enhanced driving terms near the edge of the distribution at $\sqrt{2J} \approx 1$. In particular the hollow-beam distribution shows the most dramatic excitation of resonances near the edge.

6 Conclusion

We have calculated the tune-shifts and resonance strengths for the four different distributions Gaussian, parabolic, hollow-beam and Erfc. A parameter b that characterizes the width of the distribution was chosen equal in all cases and all distributions contain equal numbers of particles. We found that the Gaussian distribution, to which we compare the others, shows the smallest tune shift and the weakest excitation of non-linear resonances. The parabolic distribution causes significantly enhanced tune-shift, but only slightly enhanced resonance driving terms. The hard edge distribution has somewhat reduced tune-shift and increased resonance driving terms, whereas the tune-shift for the hollow beam is equally weak to that of the Gaussian distribution, but has the most dramatic increase in resonance driving terms.

In conclusion we find that the Gaussian distribution is the most advantageous one, but considering that the cathodes of the electron coolers have a finite width

we have to choose from the other three distributions. There is a clear progression for the highest to lowest tune-shift going from parabolic via Erfc to hollow-beam distribution and a converse progression from largest to smallest resonance driving terms. Thus it is possible to trade a large tune-shift or large tune footprint for weaker resonance driving terms and vice-versa.

In an accelerator with very few external non-linearities due to magnetic imperfections one might be able to afford to have a large tune-shift and choose the parabolic current profile, because only the inherent non-linearities of the electron beam are driving the resonances, whereas in an accelerator with a large content of external magnetic non-linearities one would choose the hollow electron beam, because the tune spread is small and less resonances are covered by the beam distribution. The relevant criterion is the relative strength of magnetic to inherent non-linearities.

For the tune spread one has, of course, also to consider the contribution due to chromaticity and energy spread. In a cooled beam, however, that contribution should be very small or negligible.

APPENDIX

A Gaussian Distribution

The radial distribution for a Gaussian distribution is proportional to

$$\psi(r) = \frac{1}{N_0} e^{-r^2/2\sigma^2} \tag{17}$$

where σ is the rms width of the distribution and N_0 is a normalization constant that we calculate below. The corresponding electric field $E(R)$ is given by Gauss' law $2\pi R E(R) = \int_0^R 2\pi r \psi(r) dr$. Evaluating the integral and solving for $E(R)$ yields

$$E(R) = \frac{\sigma^2}{N_0 R} \left[1 - e^{-r^2/2\sigma^2}\right] \ . \tag{18}$$

The normalization constant N_0 is given by

$$N_0 = \int_0^\infty 2\pi r \psi(r) dr = 2\pi\sigma^2 \ . \tag{19}$$

When doing calculations regarding tune-shift it is convenient to normalize to the slope at the origin $R = 0$. Evaluating a Taylor-expansion of $E(R)$ around $R = 0$ we find that the slope there is

$$\frac{dE(R)}{dR}|_{R=0} = \frac{1}{4\pi\sigma^2} \tag{20}$$

B Parabolic Distribution

The representation of a parabolic distribution is given by

$$\psi(r) = \frac{1}{N_0}\left[1 - \frac{r^2}{b^2}\right] \tag{21}$$

where b is the half width of the parabolic distribution and N_0 is the normalization constant. Gauss' law yields the electric field

$$E(R) = \frac{1}{2N_0}\left[R - \frac{R^3}{2b^2}\right] \quad \text{for} \quad R \leq b \tag{22}$$

and

$$E(R) = \frac{b^2}{4N_0 R} \; . \quad \text{for} \quad R \geq b \tag{23}$$

The normalization constant evaluates to

$$N_0 = \int_0^\infty 2\pi r \psi(r) dr = \frac{\pi b^2}{2} \tag{24}$$

and the slope at zero is

$$\frac{dE(R)}{dR}|_{R=0} = \frac{1}{\pi b^2} \; . \tag{25}$$

C Hollow Beam Parabolic Distribution

The distribution of a hollow parabolic beam is given by

$$\psi r = \frac{1}{N_0}\left[1 - \frac{(r-b)^2}{a^2}\right] \tag{26}$$

where a is the half width of the parabolic rind with radius b and N_0 is a normalization constant. We need to calculate the electric filed in three regions using Gauss' law. Inside the ring we have

$$E(R) = 0 \quad \text{for} \quad R \leq b - a \; . \tag{27}$$

Within the ring we have

$$\begin{aligned} E(R) \;\; = \;\; & \frac{1}{N_0 R a^2}\left[(a^2 - b^2)\frac{R^2}{2} - \frac{R^4}{4} + \frac{2}{3}bR^3 \right. \\ & \left. -(a^2 - b^2)\frac{(b-a)^2}{2} + \frac{(b-a)^4}{4} - \frac{2}{3}b(b-a)^3\right] \\ & \text{for} \quad b - a \leq R \leq b + a \end{aligned} \tag{28}$$

and outside the ring we have

$$E(R) = \frac{4ab}{3N_0R} \quad \text{for} \quad b + a \leq R \ . \tag{29}$$

For the normalization constant we obtain

$$N_0 = \frac{8\pi}{3}ab \tag{30}$$

and for the slope at the origin we have

$$\frac{dE(R)}{dR}|_{R=0} = 0 \tag{31}$$

as could be expected.

D Erfc Distribution

The erfc distribution was introduced in Ref. [9, 10] for the investigation of the effect of smoothing the edge of an electron beam that is typically used in an electron cooler. Here we just recapitulate those results. The distribution is given by

$$\psi(r) = \frac{1}{N_0}\text{erfc}\left(\frac{r-b}{a}\right) \ . \tag{32}$$

and the corresponding electric field is calculated if Ref. [9] with the result

$$\begin{aligned} E(R) &= \frac{1}{N_0R}\Big(a^2\left[F(-b/a) - F((R-b)/a)\right] \\ &\qquad +ab\left[G(-b/a) - G((R-b)/a)\right]\Big) \end{aligned} \tag{33}$$

where the auxiliary function F and G are defined by

$$\begin{aligned} F(z) &= \int_z^\infty t\,\text{erfc}(t)dt = \left(\frac{1}{4} - \frac{z^2}{2}\right)\text{erfc}(z) + \frac{z}{2\sqrt{\pi}}e^{-z^2} \\ G(z) &= \int_z^\infty \text{erfc}(t)dt = \frac{1}{\sqrt{\pi}}e^{-z^2} - z\,\text{erfc}(z) \ . \end{aligned} \tag{34}$$

The normalization constant N_0 is given by integrating the distribution $\psi(r)$ with the result

$$N_0 = 2\pi\left[a^2F(-b/a) + abG(-b/a)\right] \ . \tag{35}$$

Finally, expanding the electric field $E(R)$ around $R = 0$ we find the slope at zero

$$\frac{dE(R)}{dR}|_{R=0} = \frac{1}{2}\text{erfc}(-b/a) \ . \tag{36}$$

References

[1] V. Parkhomchuk, et.al. *Electron Cooling for HESR, Final Report,* BINP, Novosibirsk, 2003.

[2] W. Henning (ed.), *An international Accelerator Facility for Beams of Ions and Antiprotons, Conceptual Design Report,* GSI, November 2001.

[3] E. Behtenev, et.al., *Commision of Electron Cooler EC-300 for HIRFL-CSR,* Proceedings of the European Particle Accelerator Conference in Lucerne, July 2004.

[4] D. Reistad, et al., *Measurements of Electron Cooling and "Electron Heating" at CELSIUS,* published in Proceedings of the workshop on Beam Cooling and Related Topics in Montreux, 1993, CERN 94-03, p. 183.

[5] I. Meshkov, *Electron Heating talk in Bad Bensheim,* presented at the ICFA-HB2004 workshop in Bad Bensheim, October 2004.

[6] E. Keil, *Beam-Beam Dynamics,* published in CERN Accelerator School, Rhodes, Greece, CERN 95-06, p. 539.

[7] M. Abramowitz, I. Stegun, *Handbook of Mathematical Functions,* Dover Publications, New York, 1970.

[8] W. Press, et al., *Numerical Recipes,* Cambridge University Press, Cambridge, 1986.

[9] V. Ziemann, *Resonances driven by the Electric Field of the Electron Cooler,* TSL-98-43, June 1998.

[10] V. Ziemann, *Electron Cooler driven Transverse Resonances,* contributed to the 1998 European Particle Accelerator Conference, Stockholm, Sweden.

List of Figures

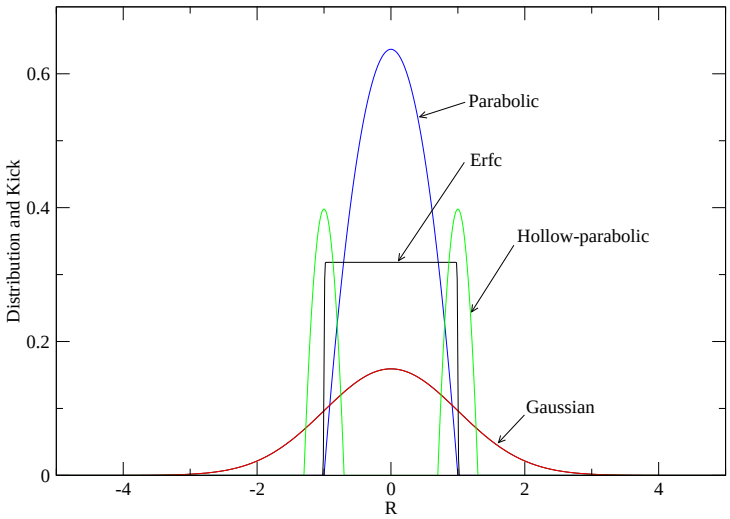

Figure 1: *The normalized charge distributions for Gaussian, parabolic, hollow-parabolic and Erfc type beams.*

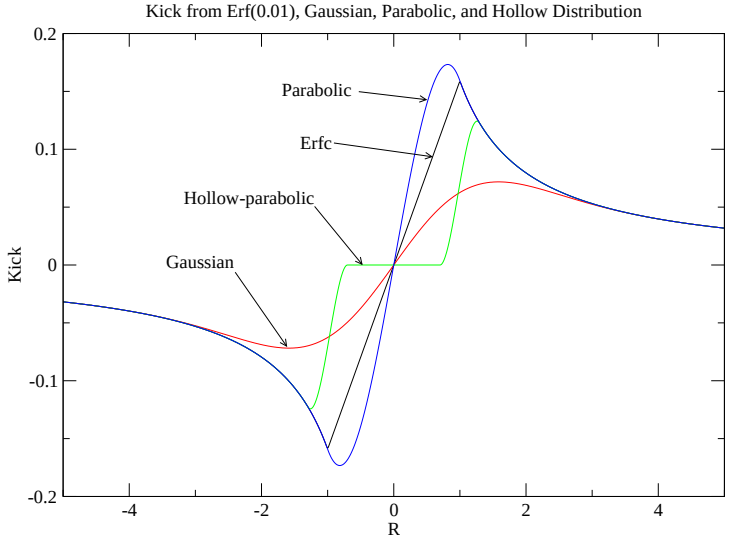

Figure 2: *The corresponding electric field from the four charge distributions.*

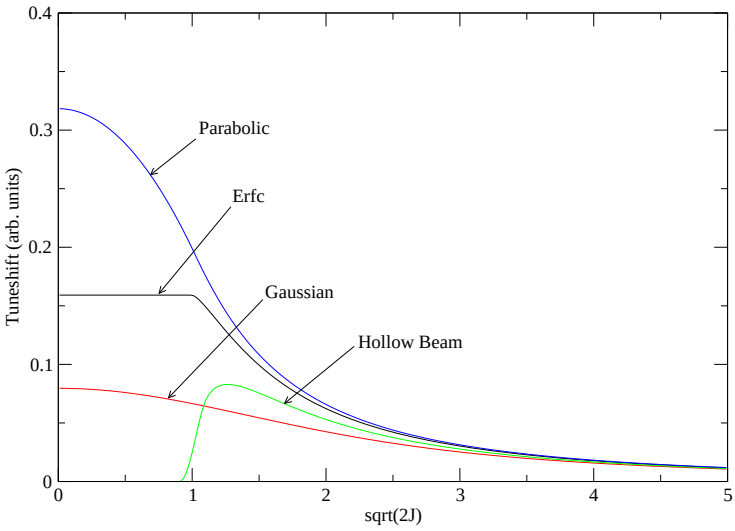

Figure 3: *Tune-shift with amplitude.*

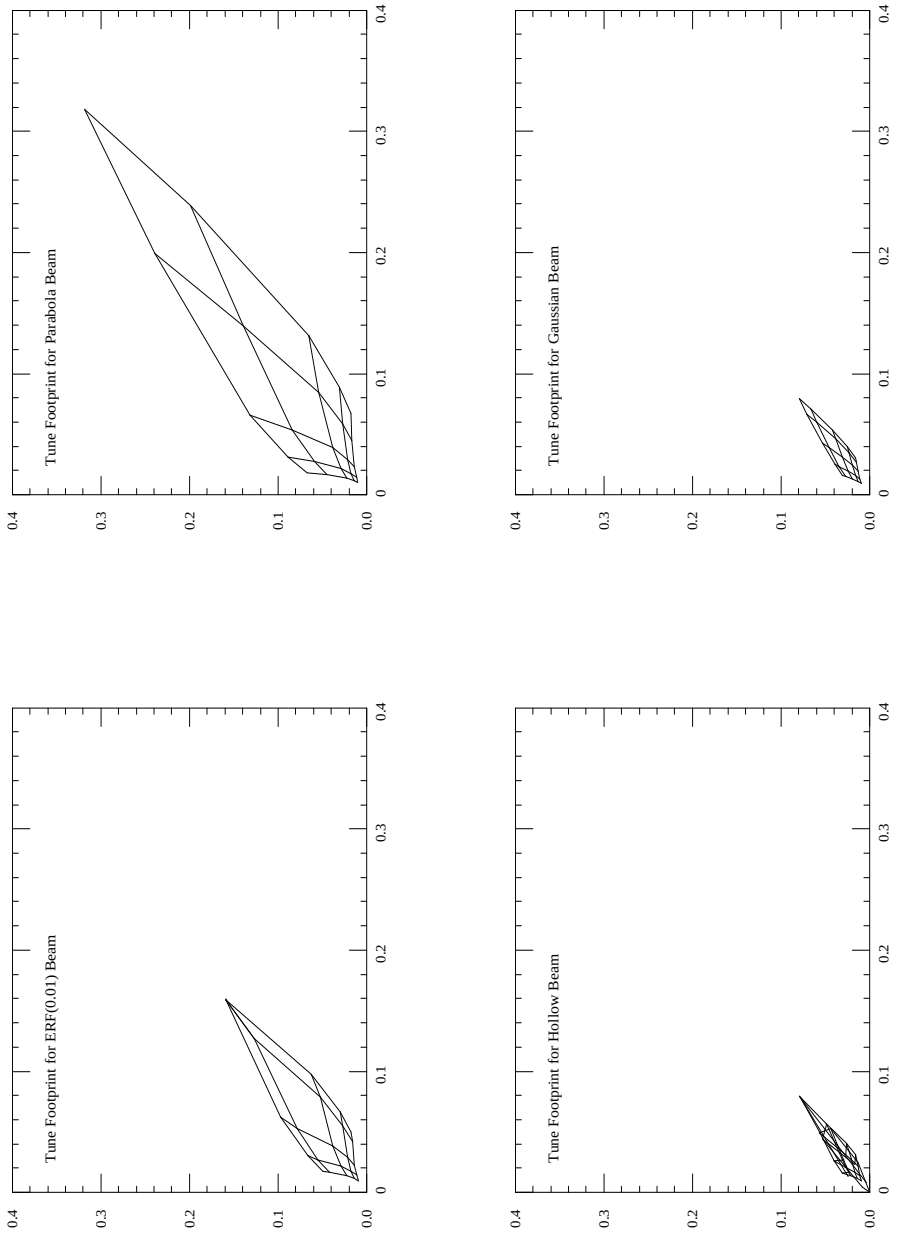

Figure 4: *The tune foot prints corresponding to the charge distributions.*

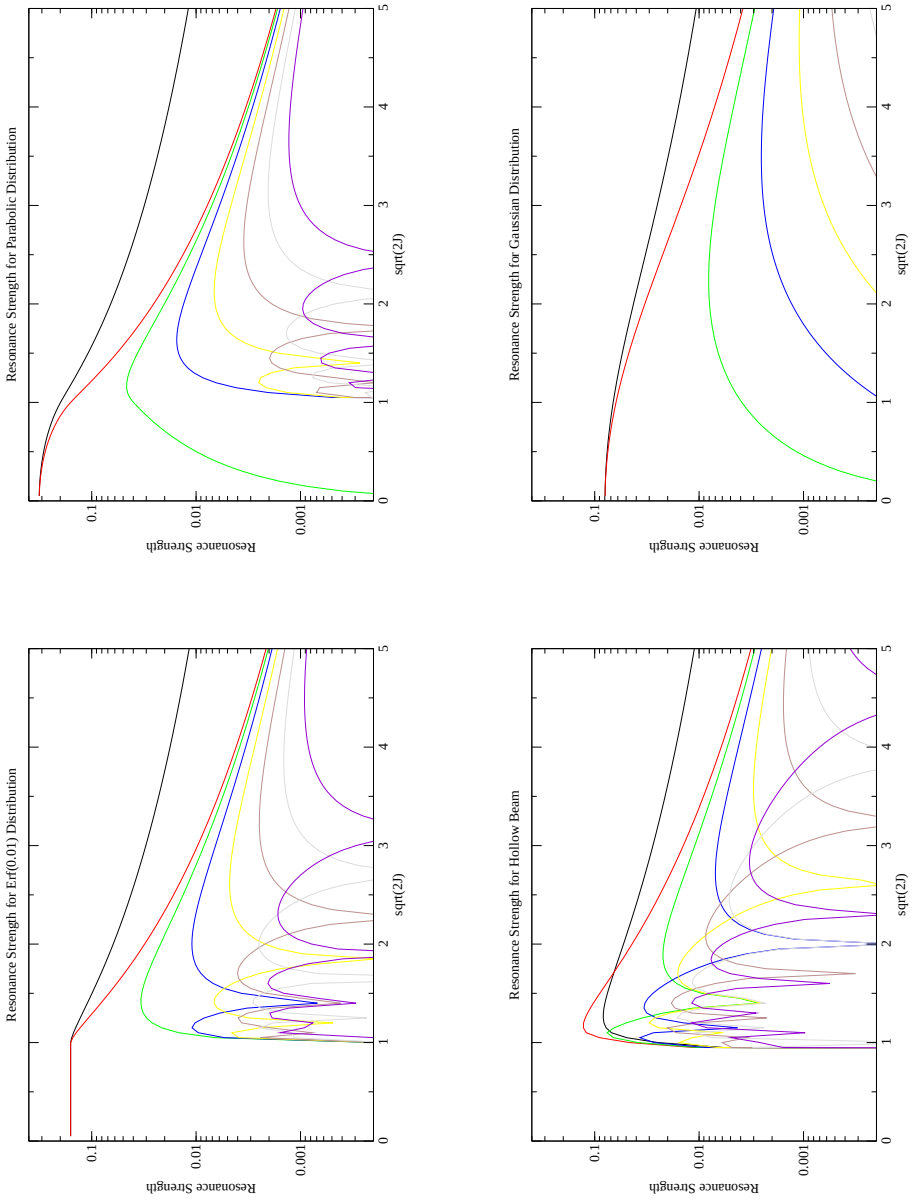

Figure 5: *The strengths of the resonances.*